A three-dimensional model of solar radiation transfer in a non-uniform plant canopy

N T Levashova, Yu V Mukhartova

Faculty of Physics, M.V. Lomonosov Moscow State University, 1 - 2, Leninskiye Gory, Moscow, 119991, Russia

E-mail: natasha@npanalytica.ru

Abstract. A three-dimensional (3D) model of solar radiation transfer in a non-uniform plant canopy was developed. It is based on radiative transfer equations and a so-called turbid medium assumption. The model takes into account the multiple scattering contributions of plant elements in radiation fluxes. These enable more accurate descriptions of plant canopy reflectance and transmission in different spectral bands. The model was applied to assess the effects of plant canopy heterogeneity on solar radiation transmission and to quantify the difference in a radiation transfer between photosynthetically active radiation PAR (=0.39-0.72 μm) and near infrared solar radiation NIR ($\Delta\lambda$ = 0.72-3.00 μm). Comparisons of the radiative transfer fluxes simulated by the 3D model within a plant canopy consisted of sparsely planted fruit trees (plant area index, PAI - 0.96 m^2 m^{-2}) with radiation fluxes simulated by a one-dimensional (1D) approach, assumed horizontal homogeneity of plant and leaf area distributions, showed that, for sunny weather conditions with a high solar elevation angle, an application of a simplified 1D approach can result in an underestimation of transmitted solar radiation by about 22% for PAR, and by about 26% for NIR.

1. Introduction

Incoming solar radiation is a key factor influencing all biological processes in Earth's biosphere. It determines the thermal regime of vegetation cover and soil, and affects the plant canopy's photosynthesis and transpiration [1]. Adequate estimation of vegetation, primary production and land surface evapotranspiration requires developing methods and models that enable highly accurate assessment of solar radiation reflection, absorption and transmission in plant canopies with non-uniform structure and diverse optical properties. During the last decades a large number of radiative transfer models based on both relatively simple parameterizations and more sophisticated approaches were developed and applied [1-9]. The most commonly used one-dimensional (1D) approaches consider the vegetation cover as a horizontally homogeneous turbid medium. They are usually based on either the "two-stream approximation" [10, 11] or a more simple approach based on the Beer–*Lambert–Bouguer* law, which assumes an exponential decrease of solar radiation depending on leaf area density [12]. It can be expected that this 1D assumption lead to uncertainties in estimation of radiation reflection, absorption and transmission in a spatially non-uniform vegetation cover. For such heterogeneous plant canopy, it is obviously necessary to use more sophisticated three-dimensional (3D) radiative transfer models that are able to take into account the 3D canopy structure [4, 8].

Within the framework of the study, a 3D radiative transfer model was developed. To quantify the effects of plant canopy heterogeneity on transfer of photosynthetically active radiation (PAR, $\Delta\lambda$ = 0.39-0.72 μm) and near infrared solar radiation (NIR, $\Delta\lambda$ = 0.72-3.00 μm) the radiative transfer

parameters simulated by the 3D model were compared with radiation fluxes simulated by a 1D approach.

2. Model description

The 3D radiative transfer model is based on the main equations and assumptions suggested by Y. Ross [1] and further developed and described by Muneni [13, 14] and Kniazikhin et al. [4, 15]. According to this approach, the distribution function of the solar radiation intensity $I_\lambda(\mathbf{r},\Omega)$ of a wavelength λ at each spatial point $\mathbf{r}=\{x,y,z\}$ inside the vegetation canopy is dependent on the solid angle $\Omega=\{\varphi,\theta\}$ and is estimated as a sum of the direct radiation $I_{m,\lambda}(\mathbf{r},\Omega)$ and scattered diffuse radiation $I_{d,\lambda}(\mathbf{r},\Omega)$, where θ is a solar zenith angle. The distribution of the direct radiation intensity inside the vegetation cover is determined from the expression $I_{m,\lambda}(\mathbf{r},\Omega)=Q_{0,\lambda}(\mathbf{r})\delta(\Omega-\Omega_0)$. The probable density of the event that the sunbeam incoming to the upper boundary of the vegetation cover along the direction Ω_0 reaches a certain point **r** inside the vegetation without being reflected or scattered by vegetation elements is defined as

$$Q_{0,\lambda}(\mathbf{r})=T_{m,\lambda}\left(\mathbf{r}-l_{\mathbf{r},\Omega_0}\Omega_0\right)\exp\left(-\int_0^{l_{\mathbf{r},\Omega_0}}\sigma(\mathbf{r}-s\Omega_0,\Omega_0)\,ds\right).$$

Here, $T_{m,\lambda}$ is intensity of direct solar radiation at the upper boundary of the vegetation cover, $l_{\mathbf{r},\Omega_0}$ is the distance between the point **r** and the upper vegetation boundary along the direction Ω_0 to the sun, $\sigma(\mathbf{r},\Omega)$ is the cross-sectional area of the interaction (scattering and absorption) of solar radiation with vegetation elements. If the uniform distribution of the leaves by the tilt angles is assumed, we can take $\sigma(\mathbf{r},\Omega)=0.5\cdot LAD(\mathbf{r})$, where $LAD(\mathbf{r})$ is the leaf area density at point $\mathbf{r}=\{x,y,z\}$.
The intensity of the scattered radiation is determined from the equation

$$(\Omega\cdot\nabla I_{\lambda,d}(\mathbf{r},\Omega))+\sigma(\mathbf{r},\Omega)I_{\lambda,d}(\mathbf{r},\Omega)=\int_{4\pi}I_{\lambda,d}(\mathbf{r},\Omega')\sigma_{s\lambda}(\mathbf{r},\Omega'\to\Omega)\mathbf{d}\Omega'+\sigma_{s\lambda}(\mathbf{r},\Omega_0\to\Omega)Q_{0,\lambda}(\mathbf{r})$$

with additional conditions on the top and the lateral borders of the vegetation cover $I_{d,\lambda}(\mathbf{r}_t,\Omega)=T_{d,\lambda}$, where $T_{d,\lambda}$ is the incoming scattered radiation into the point $\mathbf{r}_b=\{x,y,z_b\}$. At the bottom border near the soil surface, the value $I_{d,\lambda}(\mathbf{r}_b)$ is determined as $I_{d,\lambda}(\mathbf{r}_b)=\dfrac{\rho_\lambda\mu_0 Q_{0,\lambda}(\mathbf{r}_b)}{1-\rho_\lambda\pi}$ where ρ_λ is a coefficient of solar radiation reflection from the soil surface at the point $\mathbf{r}_b=\{x,y,z_b\}$ at the bottom border. In the equation for scattered radiation, $\sigma_s(\mathbf{r},\Omega',\Omega)$ is the differential cross-section for the scattering of the rays falling in the direction Ω' and scattered in the solid angle $d\Omega$ for respected r and Ω. According to Ross and Myneni [2]

$$\sigma_s(\mathbf{r},\Omega',\Omega)=\frac{1}{2\pi}LAD(\mathbf{r})\int_{2\pi^+}\left|(\Omega',\Omega_L)\right|\left(\gamma_{LD}(\Omega_L,\Omega',\Omega)+\gamma_{LS}(\Omega_L,\Omega',\Omega)\right)d\Omega_L$$

where $\gamma_{LD}(\Omega_L,\Omega'\Omega)=\begin{cases}\pi^{-1}r_{LD}(\alpha')\left|(\Omega,\Omega_L)\right|, & (\Omega,\Omega_L)(\Omega',\Omega_L)<0,\\ \pi^{-1}t_{LD}(\alpha')\left|(\Omega,\Omega_L)\right|, & (\Omega,\Omega_L)(\Omega',\Omega_L)>0,\end{cases}$ is a phase function of leaf scattering: the part of the energy intercepted by photons initially falling in the direction Ω' and scattered after collision of photons with a leaf surface with an external normal Ω_L into a solid angle

Ω; α' is an angle between the incident sunbeams and the perpendicular to the leaf surface, $r_{LD}(\alpha')$ is a hemispherical leaf reflection coefficient, $t_{LD}(\alpha')$ is a hemispherical leaf transmission function; $\gamma_{LS}(\Omega_L,\Omega',\Omega) = F_r(n,\alpha')\delta_2(\Omega,\Omega^*)$ is a mirror reflection component, where $F_r(n,\alpha') = \frac{1}{2}\left(\frac{\sin^2(\alpha'-\theta_s)}{\sin^2(\alpha'+\theta_s)} + \frac{\mathrm{tg}^2(\alpha'-\theta_s)}{\mathrm{tg}^2(\alpha'+\theta_s)}\right)$ is the air refraction index $n=1.5$, $\theta_s = \arcsin\left(\frac{\sin\alpha'}{n}\right)$, δ_2 is a Dirac delta function, Ω^* is the direction of the corresponding leaf normal for the mirror scattering of the incident and reflected rays. The intensity of solar radiation at each point $\mathbf{r}=\{x,y,z\}$ is calculated as the total intensity of the radiation flux in each of the directions determined by all possible Ω.

To solve the system of differential equations, the numerical scheme described by Ross and Myneni [2] is used.

3. Description of experimental plot and model input parameters

For numerical experiments, a one-hectare plot with sparsely planted fruit trees was chosen (figures 1-2). The height of each planted tree is 8 m, maximal diameter of a tree crown is 6 m, the distance from the ground to the crown bottom is 1 m, and diameter of a tree trunk is 0.2 m. The distance between tree trunks is 5.24 m. The total number of trees within selected plot is 181. The plant area density (PAD) includes leaf area densities (LAD) and the density of non-photosynthesizing element of trees (branches and stems). The proportion of LAD in PAD within tree crowns is changed depending on the height above a ground and the distances from the tree stem and crown edge.

The leaf area distribution inside of the tree crown is based on the model of a tree structure described by Wildowski et al. [16] and Olchev et al. [7]. The model assumes that the maximal crown spreads and LAD are observed in the upper part of the trees. Moreover, it is assumed that LAD in the tree crown decreases as the distance from tree crown edge increases. The spectral properties of the leaves and bark are taken from the literature [e.g. 17] (table 1). The modeling experiments were provided for midday hours under maximal sun height (the solar zenith angle, Θ=30° that is equal to solar elevation angle $h_\odot$=60°). It was assumed that direct portion of solar radiation is 75%.

Table 1. Reflection and transmission coefficients of plant elements and soil surface for PAR and NIR.

Spectral bands, $\Delta\lambda$ (μm)	Leaves		Branches and stems		Soil
	r_{LD}	t_{LD}	r_{LD}	t_{LD}	r_S
0.39-0.72	0.06	0.06	0.04	0.00	0.05
0.72-3.00	0.45	0.45	0.40	0.00	0.30

4. Results and discussion

The results of numerical experiments show a strong heterogeneity of radiation patterns within both the entire experimental plot and the crown of individual trees (figures 1 - 2). A strong difference in plant canopy transmission coefficients (K) between PAR and NIR is mainly governed by different reflection and transmission coefficients of leaves, bark and soil for PAR and NIR spectral bands, as well as a higher contribution of the multiple scattering from plant elements for NIR. The estimated difference of K(NIR) - K(PAR), even for relatively sparse canopy, varies between 0.02 to 0.24 (figure 3). Maximal differences are found for sites which are shaded by tree crown leaves and stems.

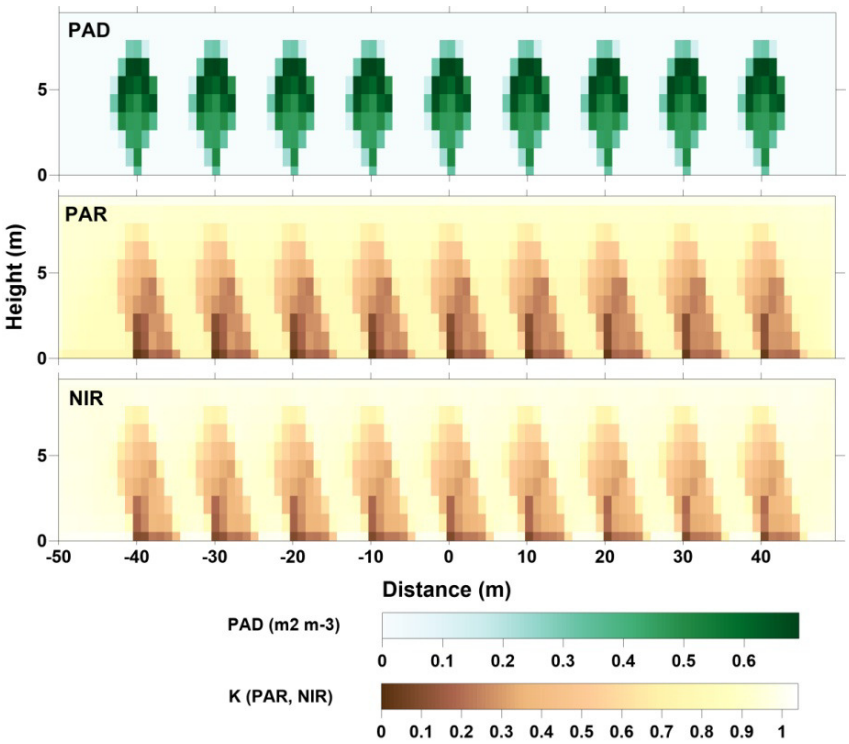

Figure 1. The distribution of plant area density (*PAD*) and the transmission coefficients (*K*) for PAR and NIR along a vertical cross-section through an experimental plot (at $y = 0$, see figure 2).

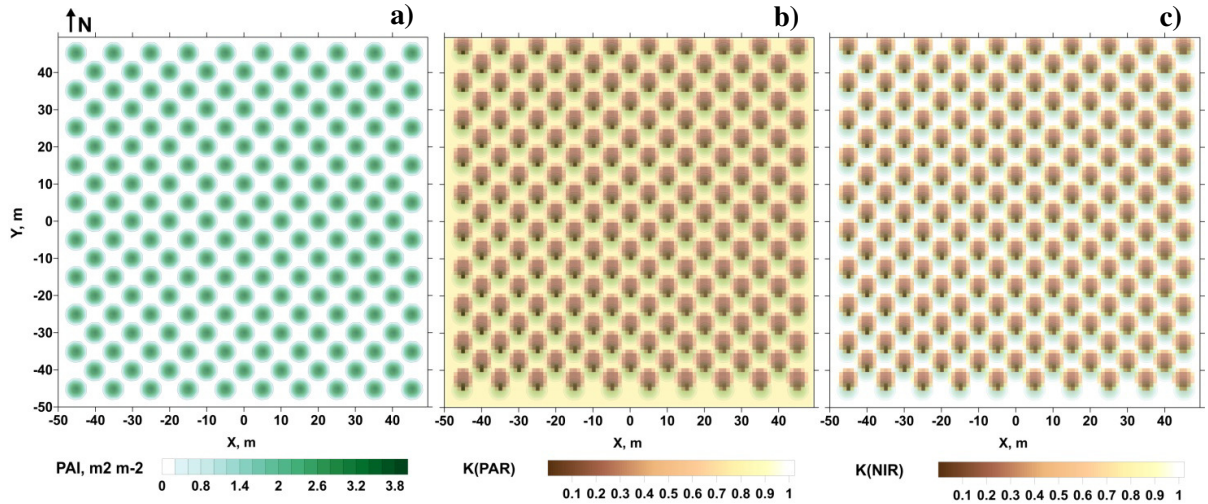

Figure 2. The distribution of the plant area index, *PAI,* (a) and the transmission coefficients (*K*) for PAR (b) and NIR (c) at a ground surface level. The shapes of tree crowns and PAI distribution are shown in the figures for *K*(PAR) and *K*(NIR) as a background.

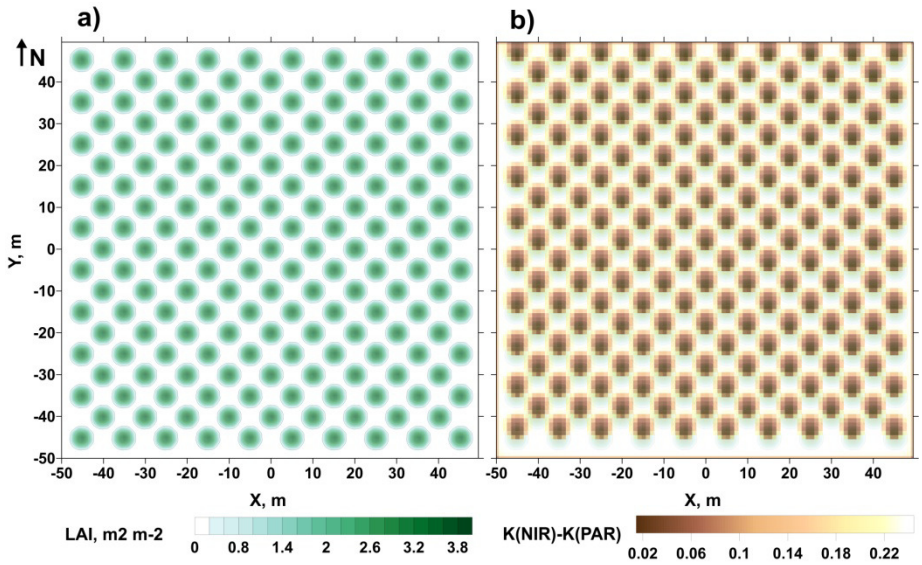

Figure 3. The distribution of *PAI* (a) and the difference between transmission coefficients *K*(NIR) and *K*(PAR) at a ground surface level (b). The shapes of tree crowns and PAI distribution are shown in the right figure for *K*(NIR) - *K*(PAR) as a background.

To estimate the possible uncertainties of solar radiation transfer estimations due to ignoring the spatial vegetation heterogeneity two separate experiments were provided. In the first experiment the solar radiation transfer was simulated for actual 3D plant canopy structure (figure 2). The second experiment imitated 1D plant canopy structure. The plant canopy in this experiment was considered as a horizontally uniform turbid medium. It was also assumed that the PAD of the plants in the experiment is dependent on vertical coordinate only. The values of PAI averaged for entire experimental plot for both modeling experiments were identical.

Comparing the extinction coefficients calculated for PAR and NIR for different levels within a plant canopy showed a significant differences in radiation flux calculations between 3D and 1D plant canopies. Transmission coefficients (K) of solar radiation predicted by the 3D model for both spectral intervals (PAR and NIR) was higher than K values calculated for 1D plant canopy for all canopy layers (tables 1-2). Maximal differences were observed for NIR at a ground surface layer (about 26%). Maximal differences for PAR were observed at 2 m layer above a ground surface. The difference between K calculated for 3D plant canopy in this layer was higher than K calculated for uniform plant canopy by about 22%. The main explanation of such differences could be the free penetration of direct solar beams through the gaps of relatively sparse 3D plant canopy. The difference between transmission of PAR and NIR can be explained by the different scattering coefficients (reflection, transmission) of the leaf and bark for PAR and NIR, as well as by contribution of the multiple scattering processes, which are due to higher leaf reflection and transmission much larger for NIR (table 1).

The modeling experiments provided by Yuan et al. [18], using the 3D radiation transfer model and the two-stream approximation model within the Community Land Model (CLM4.0), showed similar results. The canopy absorption estimated by the 3D model under low zenith angle was lower and canopy transmission was higher than in case of 1D model, due to mainly enhanced transmission through the canopy edges. In these modeling experiments, it was also shown that under the large zenith angle, the canopy absorption calculated using the 3D model can be higher than in case of 1D model, due to increases of the ground and sky shadows as well as the optical path length. Similar effects were described by Huang et al. [19] from simulation results of radiative transfer using a 3D model for a sparse forest canopy.

Table 2. Transmission coefficients (K) for PAR calculated for different levels of a horizontally uniform (1D) and heterogeneous (3D) plant canopy and averaged for entire experimental plot.

Height (m)	Transmission coefficient for vegetation with uniform structure (1D)	Transmission coefficient for vegetation of heterogeneous structure (3D)	The relative difference between K(1D) and K(3D) in %
0	0.47	0.60	-21.8
1	0.53	0.68	-22.2
2	0.52	0.67	-21.6
3	0.54	0.67	-19.0
4	0.59	0.70	-16.3
5	0.68	0.78	-13.2
6	0.80	0.88	-8.9
7	0.89	0.95	-6.8
8	1.00	1.00	0.0

Table 3. Transmission coefficients (K) for NIR calculated for different levels of a horizontally uniform (1D) and heterogeneous (3D) plant canopy and averaged for entire experimental plot.

Height (m)	Transmission coefficient for vegetation with uniform structure (1D)	Transmission coefficient for vegetation of heterogeneous structure (3D)	The relative difference between K(1D) and K(3D) in %
0	0.53	0.72	-26.3
1	0.56	0.74	-24.3
2	0.56	0.73	-23.7
3	0.58	0.73	-21.1
4	0.62	0.75	-17.0
5	0.71	0.82	-13.6
6	0.81	0.90	-10.0
7	0.88	0.96	-8.3
8	1.00	1.00	0.0

Considering the differences in radiative transfer simulations found between 1D and 3D approaches, it should be taken into account the possible uncertainties of applied 3D models arising from the model simplifications and assumptions used to describe canopy structure and radiative transfer. These uncertainties could stem from limitations of the applied numerical methods, etc. In particular, the results of a 3D radiative transfer model comparison experiment (RAMI4PILPS) provided for seven independent 3D models under controlled experimental conditions showed that the averaged deviation from predicted model parameters from some reference amounted to 19% for canopy absorption, 21% for canopy reflection and 26.7% for canopy transmission [8]. Another point that must be taken into account in a comparison of 3D and 1D models is the different complexity of applied 1D models. More sophisticated 1D radiative transfer models based, for example, on the two-stream approximation are able to describe the penetration of direct and diffuse solar radiation through the plant canopy more accurately. In this case, the difference between predicted absorbed and transmitted radiation fluxes by 3D and 1D models can be smaller.

Acknowledgement

This study was supported by a grant from the Russian Science Foundation (14-14-00956).

References

[1] Ross J 1981 *The radiation regime and the architecture of plant stands* (The Netherlands: Dr. W. Junk Publ.)
[2] Ross J and Myneni R B 1991 *Photon-Vegetation Interactions. Applications in Optical Remote Sensing and Plant Ecology* (Heidel: Springer-Verlag)
[3] Gastellu-Etchegorry J P Demarez V Pinel V Zagolski F 1996 *Remote Sens Environ.* **58** 131-156
[4] Knyazikhin Yu, Miessen G, Panferov O and Gravenhorst G 1997 *Agr. Forest Meteorol.* **88** 215–39
[5] Kuusk A and Nilson T 2000 *Remote Sens. Environ.* **72** 244–52
[6] Panferov O, Knyazikhin Y, Myneni RB, Szarzynski J, Engwald S, Schnitzler KG and Gravenhorst G 2001 *IEEE T. Geosci. Remote Sens.* **39** 241–53
[7] Olchev A, Radler K, Sogachev A, Panferov O and Gravenhorst 2009 *Ecol. Model.* **220**(21) 3046-56
[8] Widlowski J-L. *et al.* 2011 *J. Geophys. Res.* **116** G02019
[9] Widlowski J-L, Côté JF and Béland M 2014 *Remote Sens. Environ.* **142** 155-75
[10] Dickinson RE 1983 *Adv. Geophys.* **25** 305–53
[11] Olchev A, Ibrom A., Ross T, Falk U, Rakkibu G, Radler K, Grote S, Kreilein H and Gravenhorst G. 2008 *Ecol Model.* **212** 122–30
[12] Monsi M and Saeki T 1953 *Jpn. J. Bot.* **14** 22–55
[13] Myneni RB, Ross J and Asrar G 1989 *Agr. Forest Meteorol.* **45** 1–153
[14] Myneni RB, Asrar G and Gerstl SAW 1990 *Transport Theor. Stat.* **19** 205-50
[15] Knyazikhin Yu, Marshak A, and Myneni R B 2004 Three-Dimensional Radiative Transfer in Vegetation Canopies *Three-Dimensional Radiative Transfer in the Cloudy Atmosphere* ed A. Davis and A. Marshak (Berlin: Springer-Verlag) pp 617-51
[16] Wildowski J L Verstraete M Pinty B Gobron N 2003 *Allometric Relationships of Selected European Tree Species (*Italy: EC Joint Research Centre)
[17] Gates DM, Keegan HJ, Schleter JC and Weidner VR 1965 *Appl. Optics.* 4 11-20
[18] Yuan H, Dickinson RE, Dai Y, Shaikh MJ, Zhou, Shangguan W and Ji D 2012 *J. Climate* **27**(3) 1168-92
[19] Huang D, Knyazikhin Y, Wang W, Privette J, Deering DW, Stenberg P, Shabanov NV, Konstantinjva B, Myneni RB 2008 *Remote Sens. Environ.* **112**(1) 35-50